Met. Mater. Int., Vol. 18, No. 1 (2012), pp. 129~134
doi: 10.1007/s12540-012-0015-0 Published 27 February 2012

Comparative Study of the Influence of Various Melt-Treatment Methods on Hot Deformation Behavior of 3003 Al Alloy

Guiqing Chen[1,2], Gaosheng Fu[1,2,*], Hongling Chen[1], Wenduan Yan[1,2], Chaozeng Cheng[2], and Zechang Zou[2]

[1]College of Materials Science and Engineering, Fuzhou University, Fuzhou 350108, Fujian, P.R. China
[2]Department of Mechanical Engineering, Fujian Chuanzheng Communications College, Fuzhou 350007, Fujian, P.R. China

(received date: 23 March 2011 / accepted date: 14 July 2011)

3003 Al alloy samples with various metallurgical qualities were obtained by various melt-treatment methods and were deformed by isothermal compression in the deformation temperature range of 300 °C to 500 °C at strain rates between 0.0l and 10.0 s^{-1} with a Gleeble-1500 thermal simulator. The results show that there is a close relationship between melt-treatment and subsequent thermal deformation. The hot deformation activation energy (Q) bears a linear relationship with the inclusion content (H) of 3003 Al alloy prepared by various melt-treatment methods, that is $Q = 35.62\ H + 171.58$. The activation energy of the 3003 Al alloy prepared by the highly efficient melt-treatment is the lowest (174.62 $kJ \cdot mol^{-1}$), which is beneficial to the material hot plastic deformation. The critical strain of the 3003 Al alloy prepared by various melt-treatment methods is investigated through the work hardening rate. Finally, the critical conditions of the investigated alloy were determined to predict the occurrence of dynamic recrystallization.

Key words: 3003 Al alloy, melt-treatment, hot deformation activation energy, dynamic recrystallization, critical strain

1. INTRODUCTION

3003 aluminum (Al) alloy is considered as an advanced material for its excellent formability, relatively good corrosion resistance, high thermal conductivity, low density, and high strength-to-weight ratio [1-3]. It has been extensively used in containers, packaging, heat exchangers, automobile radiators, and air conditioners. To improve its performance and widen its practical application field, the mechanical properties of 3003 Al alloy have been widely studied in past decades [4-7]. Whilom Lamberigts pointed out that the excellent properties of materials can be showed only when its inner integrity reaches a certain critical level. On this basis, the role of melt treatment (such as addition of a refiner) can be brought into full play, and the mechanical properties of materials can be improved and enhanced [8]. For 3003 Al alloy, the inherent metallurgical defects, such as inclusions (Al_2O_3), stoma, and microscopic shrinkage, could damage the internal integrity of the material and further affect subsequent processing and performance. It is necessary to investigate the relationship between melt treatment and hot deformation. According to the melt-treatment principles put forward by our group, first consideration must be given to purification, exclusion of the main inclusion of Al melt, and then removal of gas. Metamorphism and refinement are based on purification. A highly efficient melt-treatment has been developed and has been widely used in Al sheet production [9].

Dynamic recrystallization (DRX) plays an important role in reducing the flow stress and grain size, and it is a powerful tool for controlling mechanical properties during the production of 3003 Al foil through hot rolling [10-13]. Occurrence of the critical condition of DRX and hot deformation active energy (Q) are important indexes to research the DRX character. The aim of this investigation is to obtain 3003 Al alloy with various metallurgical qualities by various melt-treatment methods, to discuss the relationship between metallurgical quality and hot deformation activation energy, and to establish a mathematical model of DRX critical strain and the Zener-Hollomon parameter, which is beneficial to predict and achieve desirable mechanical properties in the final product.

2. EXPERIMENTAL PROCEDURE

The materials used in this investigation were 3003 Al alloys with the following chemical compositions (all in mass fraction, %): Si 0.58, Fe 0.62, Cu 0.068, Mn 1.09, Mg 0.03, Ti

*Corresponding author: fugaosheng@fzu.edu.cn
©KIM and Springer

0.006, Zn 0.008, Ni 0.007 and balance Al. The samples used in the experiment were divided into three groups: no melt-treatment (WTC), which was original and untreated from factories; normal melt-treatment (NTC), which comprises refining and removing gas with a normal refining agent and an Al-10Ti master alloy; highly efficient melt-treatment (HTC), which comprises filtration and purification with high-efficient flux (CJ-5), Al3Ti1B1RE refinement, and M3 impurity phase modifier [14,15]. The experiment was conducted in a graphite pot resistance furnace (F97-116) with the content of 60 kg. The 110 mm×20 mm×70 mm ingots poured into a metal mould were homogenized at 510 °C for 20 h. The inclusion content was measured by means of flux flushing. The grain size of the casting ingots was measured by the linear intercept method and the average of 5 fields was taken. This was conducted using a metallography instrument (XJG-05). Cylindrical compression specimens of 15 mm in height and 8 mm in diameter were machined. Concentric annular grooves with 0.2 mm deep were machined at both end faces of the cylinders to retain the lubricant during compression testing. Graphite lubricant mixed with machine oil was used to minimize the friction between the sample and anvils. Axial-symmetry isothermal hot compression testing was carried out by means of a Gleeble-1500 dynamic hot/mechanical simulation testing machine. The deformation temperature and strain rate were within the range of 300 °C to 500 °C and 0.01 to 10.0 s^{-1}, respectively, and the deformation amount was 50% ($\varepsilon \approx 0.7$). The sample was resistance heated to deformation temperature at a heating rate of 1 °C·s^{-1} and held at that temperature for 300 s by thermocoupled-feedback-controlled AC current before compression. The deformation process was controlled by computer, and data was collected automatically.

3. RESULTS AND DISCUSSION

3.1. The inclusion and grain microstructure of 3003 Al alloy

The inclusion morphologies of the 3003 Al alloy samples are shown in Fig. 1 and purification effects are listed in Table 1. It can be seen that there are a large number of inclusions (0.6801 %) in the WTC sample, and they are larger than the inclusions of the other samples. Fewer inclusions (0.3616 %) are seen in the NTC sample, and there still are some lump inclusions. It is obvious that the number of inclusions in the HTC sample is the lowest, the amplitude of reduction is 85.78 %. At the same time, the shape of the inclusions in the HTC sample is fine, and their distribution is homogeneous, which can improve the continuity of the matrix and decrease the effect of inclusions on the material properties.

Significant changes have taken place in the casting microstructure and grain size (Fig. 2). The grain distribution is more homogeneous, and the grain size is reduced to 78 μm in the HTC sample. Since the purity of the Al melt signifi-

Table 1. Inclusion content and grain size of 3003 Al alloy

Melt-treatment processing	WTC	NTC	HTC
Inclusion content/%	0.6801	0.3616	0.0967
Removing inclusion rate/%	-	46.83	85.78
Average grain size/μm	131	92	78

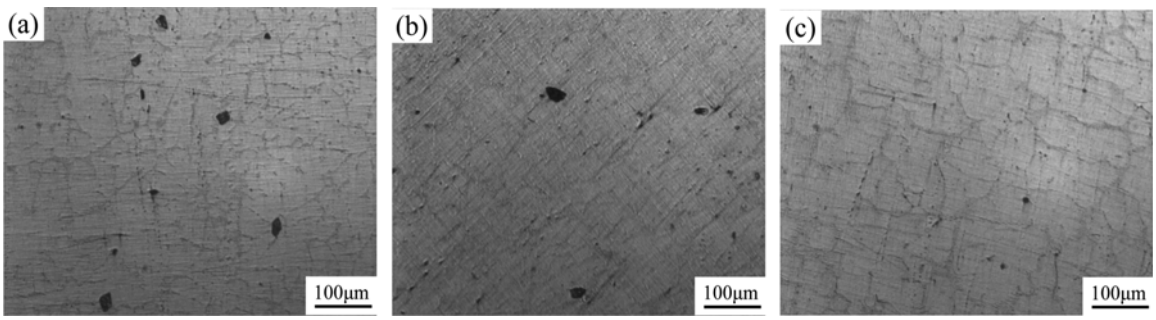

Fig. 1. Inclusion morphology of 3003 Al alloy with various melt-treatment methods: (a) WTC, (b) NTC, and (c) HTC.

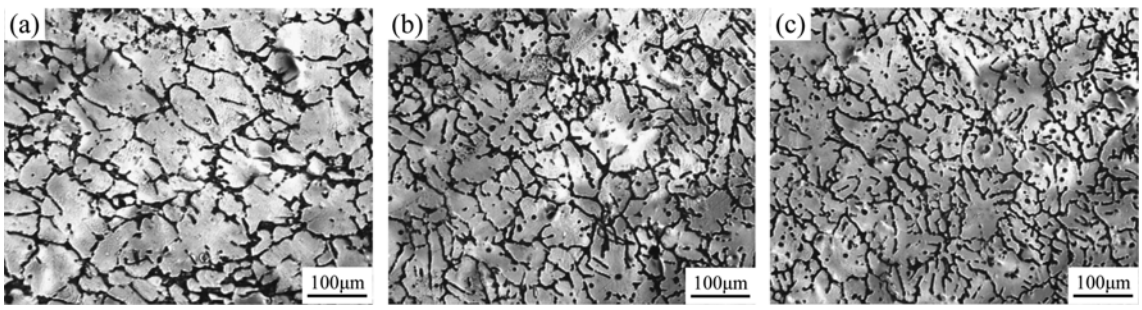

Fig. 2. Casting microstructure of 3003 Al alloy under various conditions: (a) WTC, (b) NTC, and (c) HTC.

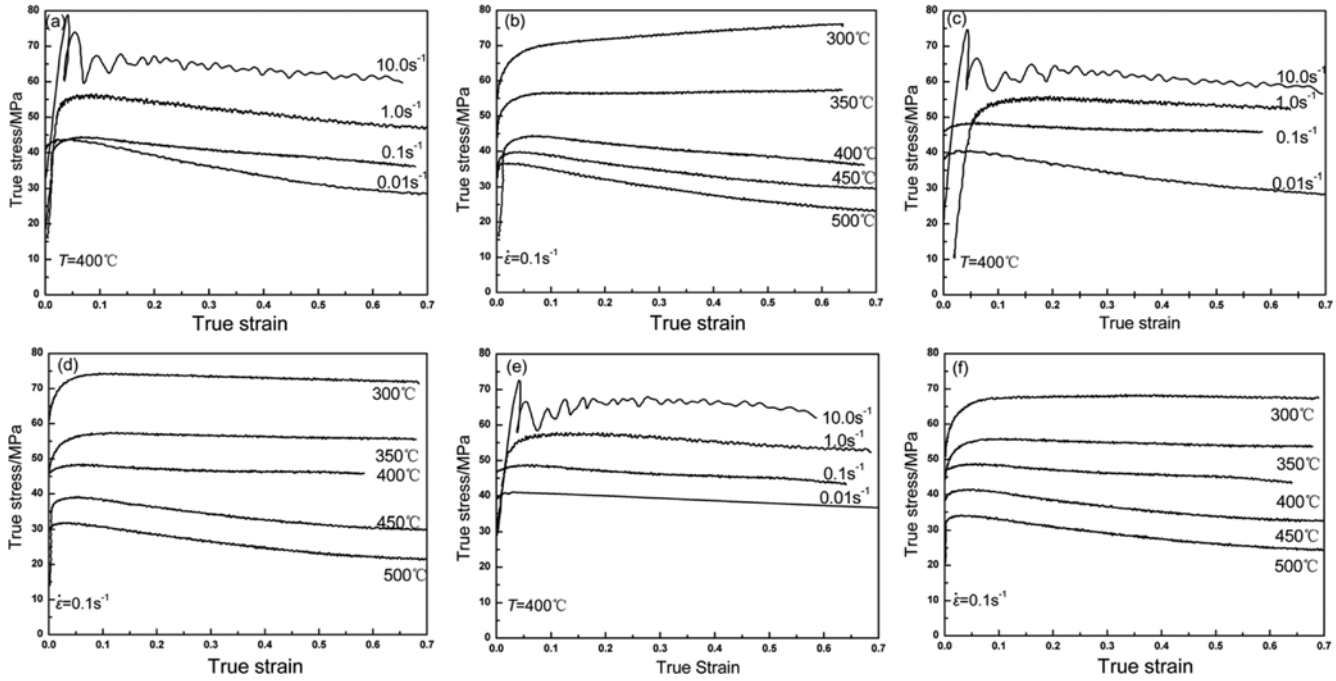

Fig. 3. Representative flow curves of 3003 Al alloy under various conditions: (a, b) WTC, (c, d) NTC, and (e, f) HTC.

cantly increased, the mobility of Al melt increased with the viscosity reduction. Some effective group element (such as TiAl3, TiB2, and RE) in a refiner or modifier can rapidly diffuse and transfer and homogeneously distribute in the Al melt, which leads to further improved refinement or metamorphism. This indicates that HTC can considerably improve the metallurgical quality of 3003 Al alloy, which is helpful for hot plastic deformation.

3.2. Analysis of hot flow curves

The influence of hot deformation conditions on the true stress-true strain curves is seen in Fig. 3. Most of the curves exhibit a peak stress followed by dynamic softening at a lower strain. Flow softening is a common characteristic of true stress-true strain curves for many alloys deformed at elevated temperatures. This can be caused by deformation heating and microstructural instabilities inside the material, such as DRX, texture formation, dynamic precipitation, and dissolution. The flow stress increases as the strain rate increases for a given strain, which suggests that 3003 Al alloy is sensitive to positive strain rate under experimental conditions. At the same time, the flow stress decreases as the deformation temperature increases at the same strain rate.

The flow stress becomes steady when a recovery process completely balances the effects of straining and work hardening at a lower temperature (≤300 °C). When the strain rate exceeds 10.0 s^{-1}, the flow stress sawtooth-shaped fluctuates, which exhibits discontinuous DRX feature. The reason is that the deformation time shortens under high strain rates. The dynamic recovery, which results from screw dislocation cross-slip and edge dislocation, is limited. Therefore, sub-boundaries do not form well. The density of dislocation in the grain remains high, and this makes the internal stored energy of the metal increase rapidly and reach DRX driving forces, leading to the occurrence of DRX. After the occurrence of DRX, there is enough time for sub-boundaries to form, which makes work hardening and dynamic softening reach a dynamic equilibrium again. Therefore, sawtooth-shaped waves are encouraged at high strain rates. In other conditions, the flow stress decreases as the strain increases after the peak, showing a DRX softening feature. Under the same hot deformation conditions, the flow stress of 3003 Al alloy with WTC is the highest, while that with HTC is the lowest.

3.3. The hot deformation activation energy of 3003 Al alloy

In hot deformation of metallic materials, it is commonly accepted that the relationship between the peak stress or steady-state stress, strain rate, and deformation temperature can be expressed as [16-19].

$$\varepsilon = A[\sinh(\sigma\alpha)]^n \exp(-Q/RT) \text{ (for all stress)} \quad (1)$$

$$\varepsilon = A_1\sigma^m \exp(-Q/RT) \ (\alpha\sigma < 0.8) \quad (2)$$

$$\varepsilon = A_2 \exp(\beta\sigma) \exp(-Q/RT) \ (\alpha\sigma > 1.2) \quad (3)$$

$$Z = \varepsilon \exp(Q/RT) \quad (4)$$

where A, A_1, A_2, n, m, β and α ($=\beta n$) are constants, Q is the activation energy for deformation, R is the gas constant (8.31 $J \cdot K^{-1} \cdot mol^{-1}$), and Z is the Zener-Hollomon parameter.

The power law, Eq. (2), and the exponential law, Eq. (3), break at a low stress and at a high stress, respectively. The hyperbolic sine law, Eq. (1), is a more general form suitable for stresses over a wide range.

Eq. (1) can be transformed as

$$\ln Z = \ln A + n\ln[\sinh(\alpha\sigma)], \tag{5}$$

$$Q = R\left[\frac{\partial \ln(\sinh(\alpha\sigma))}{\partial(1/T)}\right]_{\dot{\varepsilon}} \Big/ \left[\frac{\partial \ln(\sinh(\alpha\sigma))}{\partial \ln(\dot{\varepsilon})}\right]_{T}. \tag{6}$$

The average deformation activation energies of 3003 Al alloy prepared by various melt-treatment methods calculated by Eq. (1) to (6) in various conditions are as follows: the activation energy of WTC is 195.47 kJ·mol^{-1}, the activation energy of NTC is 185.21 kJ·mol^{-1}, and the activation energy of HTC is 174.62 kJ·mol^{-1}. It is obvious that all activation energy values are higher than that for self-diffusion in pure Al (165 kJ·mol^{-1}), suggesting that DRX occurs during hot deformation, and the deformation mechanism is mainly cross-slip of dislocations. The results correspond to the analysis of Fig. 3.

As seen in Fig. 4, the hot deformation activation energy (Q) value bears a positive linear relationship with inclusion content (H), $Q = 35.62\ H + 171.58$. The Q value can be described whether the material deformation is easy or not. It is well known that the higher the Q value, more difficult deformation is. Dislocation moving and acting reciprocally are essential for plastic deformation, which is remarkably affected by metallurgy defects of 3003 Al alloy. Therefore, the Q value would be influenced by metallurgy defects of 3003 Al alloy [20]. According to Shroh's research [21], the Q value of dislocation cross-slip can be described as $Gb^2d/5$, where G is the shear modulus, b is Burger's vector, and d is the width of the extended dislocation. It is obvious that the wider the dislocation extends, the lower the stacking fault energy, which makes it difficult for dislocation cross-slip to occur. Oxidation inclusion (Al_3O_2) is the main factor in 3003 Al alloy that blocks deformation. As seen in Table 1, the inclusion content of 3003 Al alloy with WTC is the highest, which blocks dislocation cross-slip, limits dislocation collection, and broadens the width of extended dislocation, as a result, stacking fault energy decreases, and the energy needed for slipping or climbing of the dislocations increases.

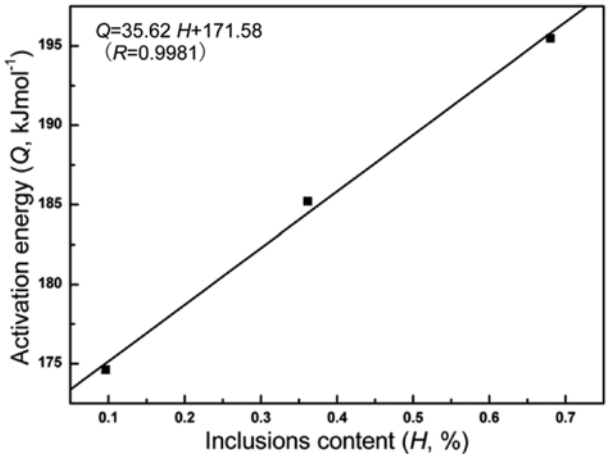

Fig. 4. The relationship between inclusion content and activation energy.

At the same time, the existence of large inclusions separates the Al matrix and hinders plastic fluid, which significantly decreases the materials plasticity and causes work hardening and brittlement to occur earlier, thus increasing the Q value. In addition, grain boundary area increases with grain size decrease, the role of grain boundary viscosity strengthens, the number of intragranular slip systems increases, and the coordination between grain slip and turn is enhanced, which causes grain boundaries to slip easily and flow stress decreases [22,23]. Also, the smaller the original grain size is, the more easily the DRX procedure can be carried out, that is£¨the smaller the steady strain value is, which lowers the Q value. Hence, melt-treatment is one of the main intrinsic factors influencing the Q value of 3003 Al alloy, and the extent of the influence of melt-treatment on Q is the result of synthetic effect of the metallurgical defects. The Q value of 3003 Al alloy with HTC is the lowest due to the improvement of its inherent metallurgical quality, which makes it deform easily.

3.4. The model of DRX critical strain

DRX critical strain (ε_c) can be determined by metallography after deformation, and it is difficult to observe and measure the extensive microstructure change. Poliak and Jonas [11,24] proposed a solution of critical strain based on the thermodynamics of irreversible processes (TIP). The critical condition corresponds to the minimum of $-\partial\theta/\partial\sigma \sim \sigma$ plot and inflexion of $\theta \sim \sigma$ plot, where θ is the strain hardening rate, $\theta = (\mathrm{d}\sigma/\mathrm{d}\varepsilon)_{\varepsilon,T}$ [25]. The $\theta \sim \sigma$ plot can well describe the microstructure changes during materials deformation and determine the characteristic value of the flow curves. When the flow stress corresponding to $\partial(-\partial\theta/\partial\sigma)/\partial\sigma = 0$ is the DRX critical stress (σ_c), it suggests that critical stress can be obtained from $(\mathrm{d}\theta/\mathrm{d}\sigma) \sim \mathrm{d}\sigma$ plots [26,27]. The $(\mathrm{d}\theta/\mathrm{d}\sigma) \sim \mathrm{d}\sigma$ plots of 3003 Al alloy in the experimental conditions are shown in Fig. 5. DRX critical stress can be determined by the minimum of the $(\mathrm{d}\theta/\mathrm{d}\sigma) \sim \mathrm{d}\sigma$ plot. The strain corresponding to the critical stress in the true stress-strain curves is critical strain.

The critical strains under various conditions can be obtained from Fig. 5 and they are listed in Table 2. It can be observed that the critical strain increases as the strain rate increases and deformation temperature decreases in the same melt-treatment conditions. The reason is that the DRX procedure is related to time; the deformation time shortens as the strain rate increases, which affects the amount of DRX nucleation and the grain growth rate because the occurrence and devel-

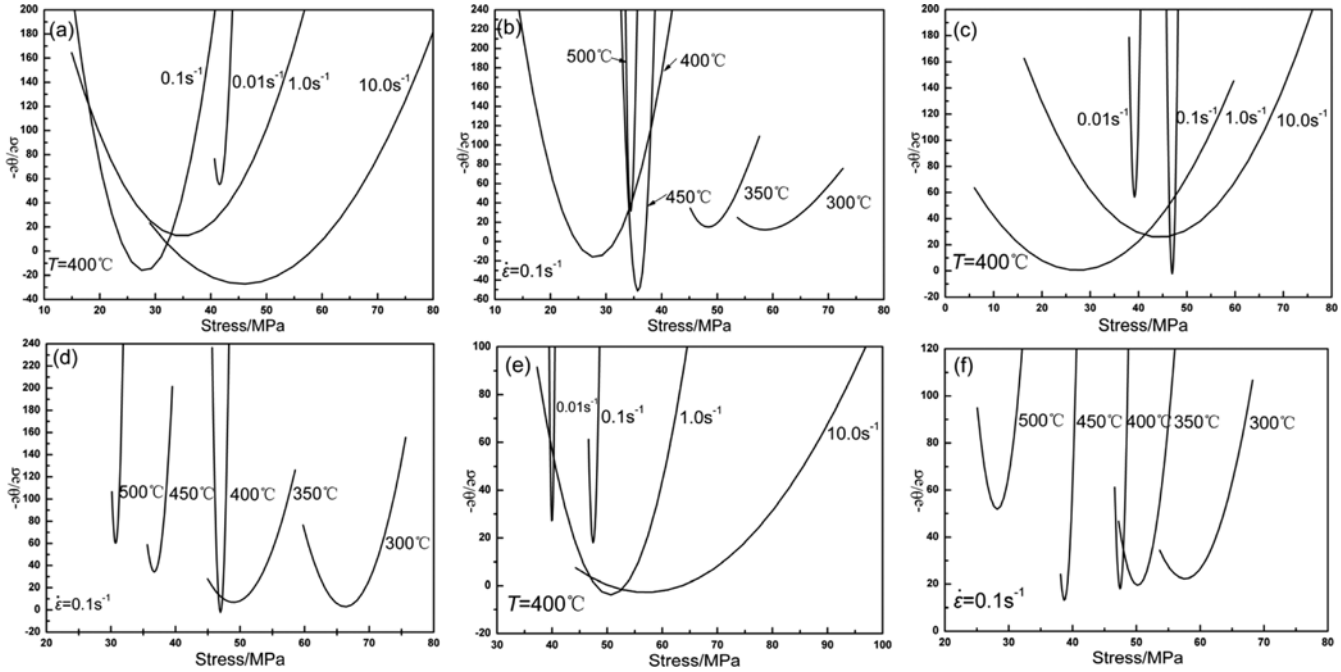

Fig. 5. The relationship between the strain hardening rate and flow stress under various conditions: (a, b) WTC, (c, d) NTC, (e, f) HTC.

Table 2. The critical strain of 3003 Al alloy ($\times 10^{-3}$)

Melt-treatment processing	T=400 °C, Strain rate (s^{-1})				$\varepsilon = 0.1s^{-11}$, Temperature (°C)			
	0.01	0.1	1.0	10.0	300	350	450	500
WTC	12.5	16.1	18.2	19.8	23.7	20.7	14.9	9.1
NTC	10.1	12.4	14.5	21.8	28.5	17.8	10.3	8.5
HTC	3.9	5.6	9.3	10.6	12.5	6.9	3.7	2.4

opment of the dislocation movement and climb are insufficient. Accordingly, the role of softening of DRX is not fully realized, which causes the critical strain to increase. On the other hand, dislocation cross-slip, climb, and subgrain formation, merger occur easily as the deformation temperature increases, which promotes the occurrence of DRX and leads to decreased critical strain [28,29]. Under the same deformation conditions, the critical strain of the 3003 Al alloy prepared by HTC is the lowest, while that of the 3003 Al alloy prepared by WTC is the highest. Since DRX is a hot activation course, the activation energy of the 3003 Al alloy prepared by HTC is the lowest. When local deformation occurs, there are many slip system startups, which makes the metal absorb much more deformation energy and reach the driving force that is sufficient for DRX to occur. At the same time, a region of high-density dislocation is formed, which results in an increase in the DRX nucleation rate. The DRX critical strain decreases, and finally, DRX occurs easily.

The Zener-Hollomon (Z) parameter is introduced to analyze the relationship between critical strain and deformation conditions. The relationship of $\ln\varepsilon_c$-$\ln Z$ obtained by linear regression of the critical strain and the Z parameter is shown in Fig. 6.

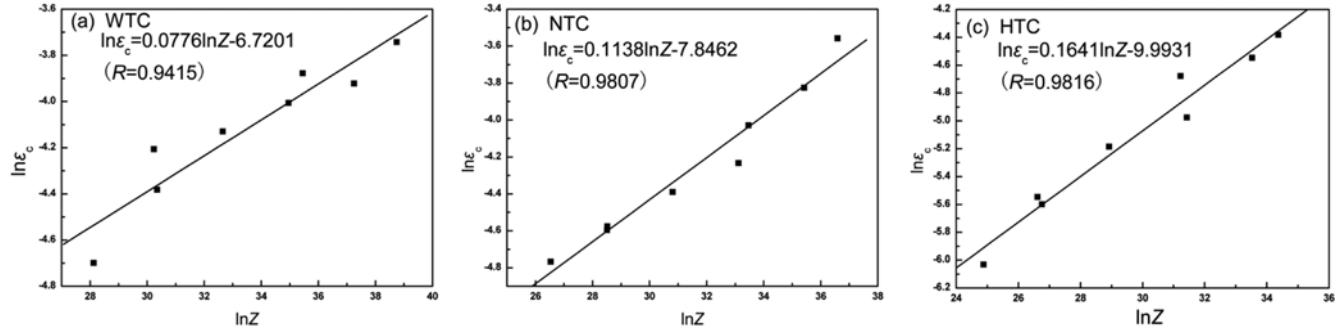

Fig. 6. The relationship between critical strain and the Z parameter.

It can be seen that the critical strain of 3003 Al alloy bears a linear relationship with Z parameter. The critical strain increases with the increase of the strain rate and decrease of the deformation temperature. The DRX critical conditions of 3003 Al alloy prepared by various melt-treatment methods can be obtained as follows: WTC is $\varepsilon_c > Z^{0.0776} + 1.2\times10^{-3}$, NTC is $\varepsilon_c > Z^{0.1138} + 4\times10^{-4}$, and HTC is $\varepsilon_c > Z^{0.1641} + 5\times10^{-5}$. The model makes it possible to calculate the critical strain of DRX occurrence as a function of temperature and strain rate for 3003 Al alloys. Therefore, the structure characteristics of 3003 Al alloy under various deformation temperatures and strain rates can be predicted and controlled, and this can provide experimental evidence to obtain the required structure and the corresponding performance to control and optimize hot plastic deformation conditions.

4. CONCLUSIONS

1. Efficient melt-treatment technology can significantly improve the internal metallurgical quality of 3003 Al alloy, decreasing inclusion content and improving the microstructure. Therefore, attention should be paid to the influence of melt-treatment on subsequent thermal deformation.

2. The hot deformation activation energy (Q) of 3003 Al alloy bears a linear relationship with the inclusion content (H), $Q = 35.62\ H + 171.58$. The activation energy of 3003 Al alloy prepared by the highly efficient melt-treatment is the lowest, 174.62 kJ·mol^{-1}. Its inherent metallurgical quality is significantly improved, which is advantageous for hot plastic deformation of the alloy.

3. Under the same hot deformation conditions, the critical strain is related to the melt-treatment process, and the critical strain of 3003 Al alloy prepared by the highly efficient melt-treatment is the lowest. Finally, the critical conditions of DRX occurrence are achieved.

ACKNOWLEDGMENTS

This work is supported by the Educational Commission of Fujian Province of China (Grant No. JA08249) and the Natural Science Foundation of Fujian Province of China (Grant No. E0610004).

REFERENCES

1. B. Luan, T. Le, and J. Nagata, *Surf. Coat. Technol*. **186**, 431 (2004).
2. R. Salghi, L. Bazzi, B. Hammouti, A. Bendou, A. Addie, and S. Kertit, *Prog. Org. Coat*. **51**, 113 (2004).
3. J. Lacaze, S. Tierce, M. C. Lafont, Y. Thebault, N. Pébère, G. Mankowski, C. Blanc, H. Robidou, D. Vaumousse, and D. Daloz, *Mater. Sci. Eng. A* **413-414**, 317 (2005).
4. H. W. Huang, B. L. Ou, *Mater. Sci. Eng. A* **30**, 2685 (2009).
5. C. L. Yeh, Y. F. Chen, C. Y. Wen, K. T. Li, *Thermal Fluid Sci*. **27**, 271 (2003).
6. G. A. Zhang, L. Y. Xu, Y. F. Cheng, *Corros. Sci*. **5**, 283 (2009).
7. W. C. Liu, T. J. Zhai, and G. Morris, *Scripta Mater*. **51**, 83 (2004).
8. M. Lamberigts, G. Walmag, D. Cotsouradis, P. Delneuville, and M. Meeus. *AFS Transactions* **93**, 569 (1985).
9. G. S. Fu, W. Z. Chen, K. W. Qian, and J. X. Kang. *Foundry Technol.* **24**, 546 (2003).
10. J. J. Jonas, *Mater. Sci. Eng. A* **184**, 155 (1994).
11. E. I. Poliak and J. J. Jonas, *Acta Mater*. **44**, 127 (1996).
12. G. R. Stewart, J. J. Jonas, and F. Montheillet, *ISIJ Int*. **44**, 1581 (2004).
13. S. H. Cho, S. I. Kim, and Y. C. Yoo, *J. Mater. Sci. Lett*. **16**, 1836 (1997).
14. G. S. Fu, W. Z. Chen, and K. W. Qian, *The Chinese J. Nonferrous Met.* **12**, 269 (2002).
15. G. S. Fu, F. S. Sun, L. Y. Ren, W. Z. Chen, and K. W. Qian, *J. Rare Earths* **20**, 61 (2002).
16. J. R. Cho, W. B. Bae, W. J. Hwang, and P. Hartley, *J. Mater. Process. Tech*. **118**, 356 (2001).
17. E. Cerri, S. Spigarelli, E. Evangelista, and P. Cavaliere, *Mater. Sci. Eng. A* **324**, 157 (2002).
18. S. Spigarelli, E. Evangelista, and H. J. Mcqueen, *Scr. Mater.* **179**, 49 (2003).
19. F. Bardi, M. Cabibbo, E. Evangelista, S. Spigarelli, and M. Vukcevic, *Mater. Sci. Eng. A* **339**, 43 (2003).
20. G. S. Fu, W. D. Yan, H. L. Chen, G. Q. Chen, and B. Ma, *Special Casting & Nonferrous Alloys* **29**, 604 (2009).
21. J. J. Jonas, C. M. Sellars, and W. J. Mcg, *Metall. Reviews* **130**, 1 (1969).
22. M. Enomoto, *Met. Mater. Int*. **4**, 115 (1998).
23. Y. S. Lee, D. W. Kim, D. Y. Lee, and W. S. Ryu, *Met. Mater. Int*. **7**, 107 (2001).
24. E. I. Poliak and J. J. Jonas, *ISIJ Int*. **43**, 684 (2003).
25. N. Christodoulou and J. J. Jonas, *Acta Metallurgica* **32**, 1655 (1984).
26. A. Manonukul and F. P. E. Dunne, *Acta Mater*. **47**, 4339 (1999).
27. S. I. Kim and Y. C. Yoo, *Mater. Sci.Technol*. **18**, 160 (2002).
28. M. M. Myshlyaev, H. J. Mcqueen, A. Mwembela, and E. Konopleva, *Mater. Sci. Eng. A* **337**, 121 (2002).
29. A. Mwembela, E. B. Konopleva, and H. J. Mcqueen, *Scripta Mater*. **37**, 1789 (1997).